Journal of New Technology and Materials(JNTM)
J. New Technol. Mater.
Vol. 07, N°02 (2017)30-37

OEB Univ. Publish. Co.

Structure, morphology and bioactivity of bioactive glass derived xerogel and aerogel

Dalila Ksouri[a], Hafit Khireddine[a], Ali Aksas[a], Tiago Valente[b], Fatima Bir[a], Nadir Slimani[a] and José Domingos Santos[b]

[a]*Laboratoire de Génie de l'Environnement (LGE), Faculté de Technologie, Département de Génie des Procédés, Université de Bejaia, 06000 Bejaia, Algerie*

[b]Department ofMaterials, Faculty of Engeneering, University of Porto (FEUP), Portugal

Corresponding author: email:dalidakso@gmail.com

Received date: March 03, 2017; accepted date: Dec 16, 2017

Abstract

Xerogel and aerogel ternary bioactive glasses (SiO_2-CaO-P_2O_5) have been prepared by sol-gel method. The xerogel bioactive glass was synthesized by heating a solution of precursors in ethanol at 60°C and dried at 130°C. Whereas, the aerogel bioactive glass was prepared by autoclaving an identical solution at supercritical conditions of ethanol solvent (BG-AGE) and the final products were sintered at 600°C. Moreover, the influence of two solvents acetone and methanol on the structure and morphology of the aerogel bioactive glasses was also studied.

After the synthesis of bioactive glasses powders, the bioactivity test was performed; their structure and morphology were distinguished by different analysis methods XRD, FTIR and SEM – EDS. The XRD analysis showed the amorphous structure of the powders before the immersion in SBF solution and the crystal structure of hydroxyapatite after one day of immersion for aerogels bioactive glass and three days for xerogel bioactive glass. The EDS analysis showed the presence of Si, Ca and P component of the bioactive glasses and in the SBF solution the Si decreased and the Ca and P increased according to the period of immersion which improves the formation of an apatite layer.

Keywords: Biomaterials; Bioactive glass; Sol-gel method; Xerogel; Aerogel; Bioactivity.

1. Introduction

Bioactive glasses have been investigated since the initiating work by Hench et al. in 1972 with the formulation (CaO-P_2O_5-SiO_2) [1]. The bioactive glasses constitute an important group of biomaterials that have wide application in regenerative medicine. This family of substitutes is particularly suitable for filling bone defects [2], prosthetic coatings in orthopedic surgery, maxillofacial, aestheticians and dental [3 - 5]. They are also applied to compensate an organ or deficient tissue in pathology, trauma or aging tissues [6, 7].

In fact, in contact with living tissues, bioactive glasses generate a series of physical and chemical reactions to material/bone tissue leading to the formation of hydroxy-carbonate apatite (HCA) layer interface [8, 9], which has a similar composition to the inorganic part of human bones [10, 11]. However, the method ofpreparation ofbioactive glassesgreatly influencesthe results of theirbioactivity.Sol-gel is the most widely used technique for the synthesis of bioactive glasses. The bioactive glasses derived from Sol-Gel, compared to traditional melt processed, have higher bioactivity and biodegradability [5]. When the liquid from the gel is evaporated at room temperature, the solid gels left behind are called xerogels. Whereas, when the liquid from the gel is extracted at supercritical state of liquid, these materials are called aerogels. Aerogels are generally monolithic and have lower density and shrinkage than xerogels [12, 13]. Most of the bioactive glassesarepreparedfromxerogel.

The aim of this investigation is the development of ternary bioactive glasses (SiO_2-CaO-P_2O_5)fromxerogelandaerogel using different solvents through sol-gel method. This work is divided in two main. The first is the characterization of all the powders with different analysis methods to distinguish the differences in their structures and morphologies. The second is the test of their bioactivity by immersion in simulated body fluid (SBF) solution to analyze its feasibility as a biomaterial.

2. Materials and methods

2.1. Materials

Tetraethylorthosilicate (TEOS), calcium nitrate tetrahydrate$Ca(NO_3)_2.4H_2O$, triethyl phosphate (TEP) as starting materials for the preparation of bioactive glass, ethanol C_2H_5OH, Methanol CH_3OH, Acetone C_3H_6O as solvents and hydrochloric acid HCl 2N as catalyst [14]. All the reagents necessary to prepare the solution of SBF according to the protocol of Kukoubo [15] were used for the test of bioactivity.

2.2. Preparation of bioactive glass powders

The sol gel technique was used to prepare the ternary bioactive glass SiO_2-CaO-P_2O_5 [10,]. Initialy, the tetraethylorthosilicate (TEOS) was added to ethanol as an alcoholic medium and the mixture was stirred for 30 min. The following reagents were added in the following sequence, stirring 30 min for each reagent to react completely: the H_2O:TEOS molar ratio was 4:1, triethylphosphate (TEP), calcium nitrate tetrahydrate andhydrochloric acid (HCl, 2N). After the final addition, the solution was stirred for one more hour.For the xerogel bioactive glass (BG-XG), the solution was heated at 60°C for 10 h and dried at 130°C for 20 h. Another solution was autoclaved at supercritical conditions of ethanol solvent (pressure of 63 bars, temperature of 243°C) to obtain an aerogel bioactive glass (BG-AGE). To see the influence of the solvent on the structure and morphology of the aerogel bioactive glass, two others solutions were autoclaved at supercritical conditions of acetone solvent (pressure of 47 bars, temperature of 235°C) (BG-AGA)and methanol solvent (pressure of 79 bars, temperature of 240°C) (BG-AGM). The obtained products (xerogel and aerogels) were crushed and sintered at 600°C for 2h.

2.3. In vitro bioactivity

The different bioactive glass powders were crushed and sieved less than 38 µm and pressed into pellets of 15 mm in diameter and 2 mm in thickness) were used to test their in vitro bioactivity. The pellets were soaked into simulated body fluid (SBF) solution prepared according to the protocol developed by Kokubo et al. [15] at 37°C for 1, 3 and 7 days with a surface area to volume ratio of 0.1 cm^{-1} [16]. The pH of SBF solution used is buffered at 7.4 with Tris buffer and hydrochloric acid. The SBF solution of the soaking samples was refreshed every two days. After being soaked, the pellets were extracted from the solution, rinsed with deionized water and dried at room temperature. The pellets without soaking in SBF are termed as zero day (0 d). The formation of an appatite- like layer on the surface of specimens was investigated by XRD for phase analysis, scanning electron microscopy (SEM) for morphology and energy dispersive spectroscopy (EDS) for elemental analysis.

2.4. Characterization

2.4.1. Elemental composition analysis

The elemental composition of bioactive glass particles was confirmed by energy dispersive X-ray analysis (EDS) technique (detector SUTW-SAPPHIRE, resolution: 125.01).

2.4.2. X-ray diffraction

X-ray diffraction (XRD) of the samples was conducted on a Bruker D8 Discover with Cu-Kα radiation (λ=1,54060Å) at 40 kV and 40 mA. X-ray diffraction diagrams were recorded in the interval 2 Theta between 10° and 80° at a scan speed of 0.04°/s.

2.4.3. Fourier transforms infrared spectroscopy

The powders were examined by Fourier transforms infrared spectroscopy with IR Affinity-1 SHIMADZU spectrometer. For IR analysis in the first 2% (weight %) of the powders were carefully mixed with 98% of KBr and pelletized under vacuum. Then the pellets were analyzed in the range of 400 to 4000 cm^{-1} at the scan speed of 40 scan / min with 4 cm^{-1} resolution.

2.4.4. Scanning electron microscopy (SEM)

The surface microstructure of the samples was performed using a High resolution (Schottky) Environmental Scanning Electron Microscope with X-Ray Microanalysis and Electron Backscattered Diffraction analysis: Quanta 400 FEG ESEM / EDAX Genesis X4M.
Samples were coated with Au/Pd thin film, by sputtering, using the SPI Module Sputter Coater equipment.

3. Results

3.1. Characterization of different bioactive glasses

3.1.1. Elemental composition

The elemental composition of bioactive glasses obtained by EDXS microanalysis presented in Fig 1, shows the quantitative EDXS analysis spectrum, which confirms the presence of all the species introduced during the mixing step of the sol-gel process either for the xerogel or aerogel. Peaks observed at 1.75, 2 and 3.7 represent Si, P and Ca respectively indicating the consisting elements of ternary bioglass[17 - 19].
The atomic percentage of the different bioactive glass powders are shown in Table 1. We noticed that the

percentage of the elements Si and P are higher in the case of aerogels bioactive glass unlike to the Ca which was higher in xerogel bioactive glass. This is certainly generated by condensation of silanol groups and the elimination of the remaining nitrates and organic compound from the precursors.

Table 1. Composition of bioactive glass powders by EDXS

Elements	C	O	Si	P	Ca
BG-XG	8.67	58.59	20.20	2.61	9.93
BG-AGE	4.23	59.48	24.96	4.08	7.24
BG-AGA	4.35	61.09	24.89	3.24	6.43
BG-AGM	4.29	60.95	25.36	3.37	6.03

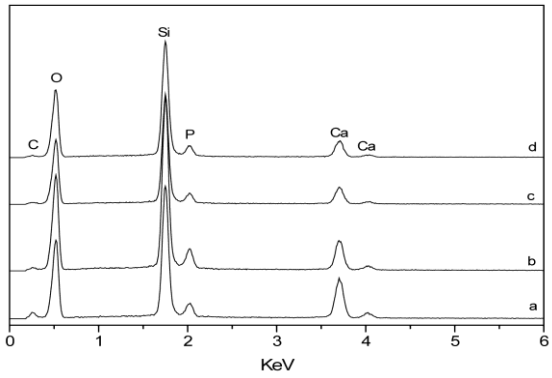

Fig. 1. *The quantitative EDXS analysis spectrum of bioactive glass powders: a- XG-BG 600°C, b- AGE-BG 600°C, c- AGA-BG 600°C and d- AGM-BG 600°C.*

3.1.2. X-ray diffraction analysis

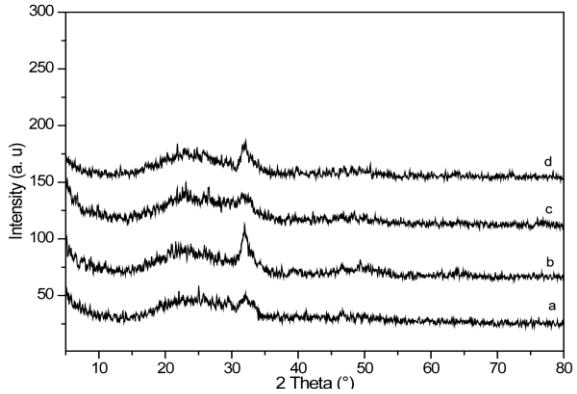

Fig. 2. *XRD pattern of bioactive glass powders: a- XG-BG 600°C, b- AGE-BG 600°C, c- AGA-BG 600°C and d- AGM-BG 600°C.*

The X-ray diffraction analysis results of bioglasses are shown in Fig 2. Here we can see that the xerogelbioglass (a) and aerogels bioglasses (b), (c) and (d), show the same paterns. These samples take amorphous state indicative of the intern disorder and glassy nature of these materials [14, 20]. At the same time one small peak with weak intensity at the position 32° can be assigned to the wollastonite ($CaSiO_3$) or to the apatite [21 - 23].

3.1.3. Infrared spectra of bioactive glasses

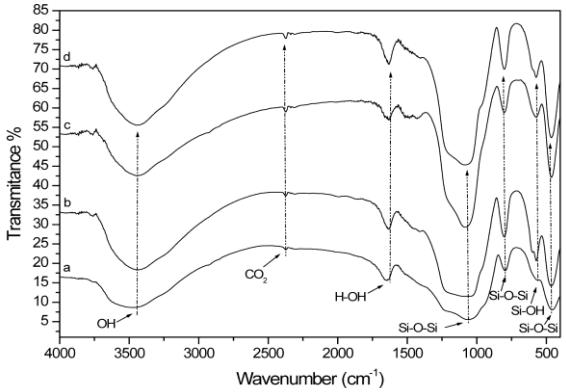

Fig. 3. FTIR spectra of bioactive glass powders: a- XG-BG 600°C, b- AGE-BG 600°C, c- AGA-BG 600°C and d- AGM-BG 600°C.

The formation of xerogel and aerogels bioactive glass was further confirmed by FTIR spectral analysis, which is shown in Fig 3. The samples shown a strong adsorption bands at 1036 – 1082 cm^{-1} assigned to the Si-O-Si asymmetric bond stretching vibrations, the bond in the 785 – 790 cm^{-1} regions is attributed to the symmetric Si-O-Si stretching vibrations [4, 5, 7, 20, 23] and the absorption around 453 – 463 cm^{-1} due to the vibrational mode of the bending of Si-O-Si [22 - 27] which prove that all the samples are mainly composed of a Si-O-Si network. The spectra involve also the band around 956 cm^{-1} attributed to the stretching vibrations of Si-OH bonds [24, 28, 29].The weak inflection at 1620-1653 cm^{-1} and the broad band centered at 3438-3455 cm^{-1} are assigned to O-H band of adsorbed water and structural hydroxyl group respectively [4, 5, 30] and finally the band at 2372 cm^{-1} is attributed to adsorption of CO_2 by the atmosphere [7].

3.1.4. Structure and morphology of bioactive glass powders

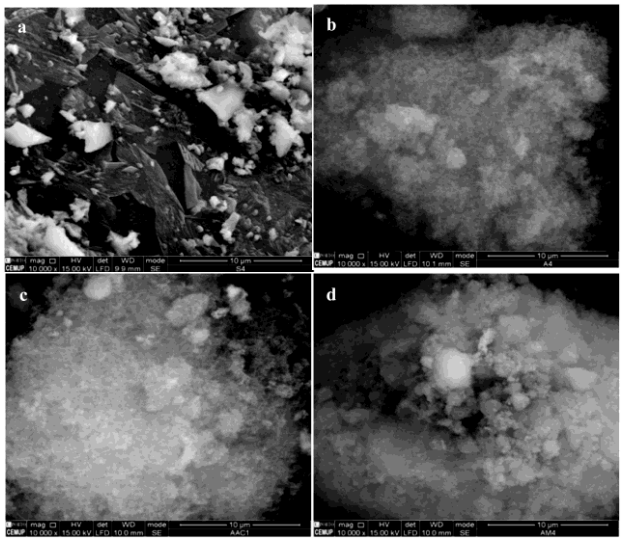

Fig. 4. SEM micrographs of bioactive glass powders: a- XG-BG 600°C, b- AGE-BG 600°C, c- AGA-BG 600°C and d- AGM-BG 600°C.

The SEM micrographs of the xerogel and aerogel bioactive glass are shown in Fig 4. Aerogel bioactive glass particles were noticed to be mostly spherical with a spongy structure and a size of nonmetric, in contrast to the xerogel bioactive glassswhich isconstituted of asingleblock. SEM images also show that the obtained aerogels bioactive glass are less dense and more porous in comparison to the xerogel bioactive glass.

Comparing between the three aerogels bioactive glass powders, it is noticed that the aerogel prepared with the ethanol solvent is less dense than the two others and the aerogel prepared with the solvent methanol is most dense with the appearance of spherical aggregates. This difference is probably due to the alkyl group in the case of ethanol and methanol solvent and to the functional group in the case of acetone.

3.2. In vitro assays

3.2.1. X-ray diffraction analysis

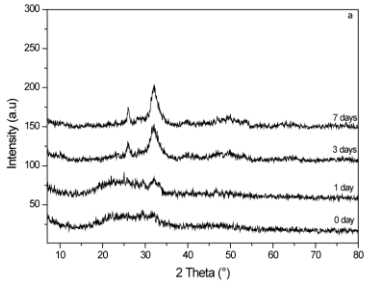

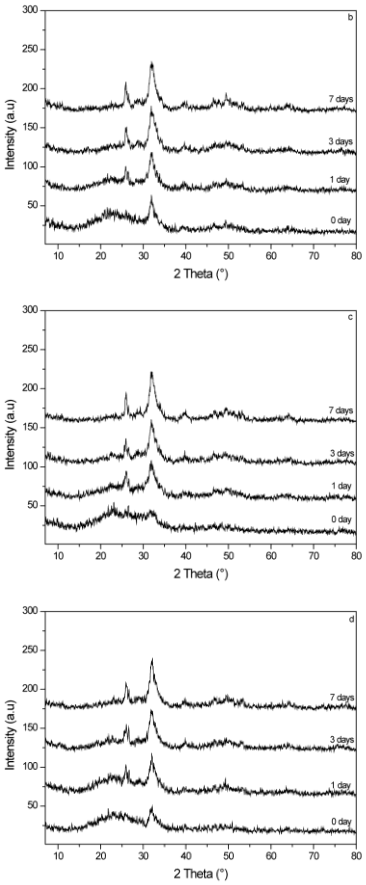

Fig. 5. XRD pattern of bioactive glass powders before and after soaking in SBF solution for 0, 1, 3 and 7 days: a- XG-BG 600°C, b- AGE-BG 600°C, c- AGA-BG 600°C and d- AGM-BG 600°C.

Fig. 5 shows the XRD patterns of bioactive glass pellets prepared from xerogel and aerogels before and after soaking in SBF solution for 0, 1, 3 and 7 days. The results indicate that all the pellets prepared either with xerogel or aerogels bioactive glass possess bioactivity. The XRD pattern shows two diffraction peaks at 26 and 32° (2θ) corresponding to (002) and (211) reflections of an apatite phase [19, 27]. These peaks are observed after one day for aerogels bioactive glass pellets BG-AG (Fig 5 b-d) and after 3 days for xerogel bioactive glass BG-XG (Fig 5 a). These results indicate that an apatite crystal was deposited on the surface of the pellets. However, the diffraction peaks are less defined for BG-XG which may be due to a lower thickness of the calcium phosphate layer.

3.2.2. Elemental composition by EDXS Analysis

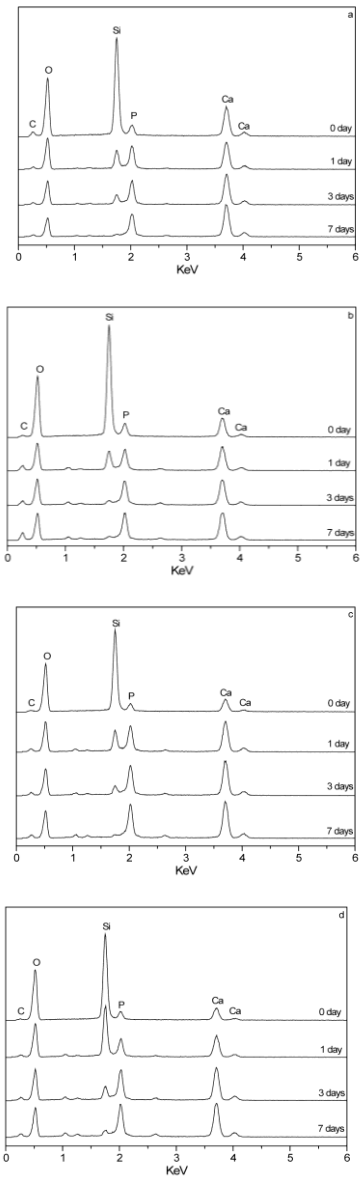

Fig. 6. The quantitative EDXS analysis spectrum of bioactive glass pellets before and after soaking in SBF solution for 0, 1, 3 and 7 days: a- XG-BG 600°C, b- AGE-BG 600°C, c- AGA-BG 600°C and d- AGM-BG 600°C.

Elemental analysis of bioactive glass pellets before and after soaking in SBF for 0, 1, 3 and 7 days are shown in Fig 6. The EDXS analysis was done for a surface of 150 µm. The results show a remarkable increase of the intensity of the elements calcium and phosphorus and reduction of the silica in all the pellets from the first day of immersion in SBF solution except the aerogel bioactive glass pellets prepared with the methanolsolvent, which shows a slight difference compared to those without immersion 0 day. After 7 days of immersion we noticed the almost total disappearance of element Si and the appearance only of elements Ca and P which confirm that the surfaces of the pellets are covered by an apatite layer.

3.2.3. Structure and morphology of bioglasses by SEM

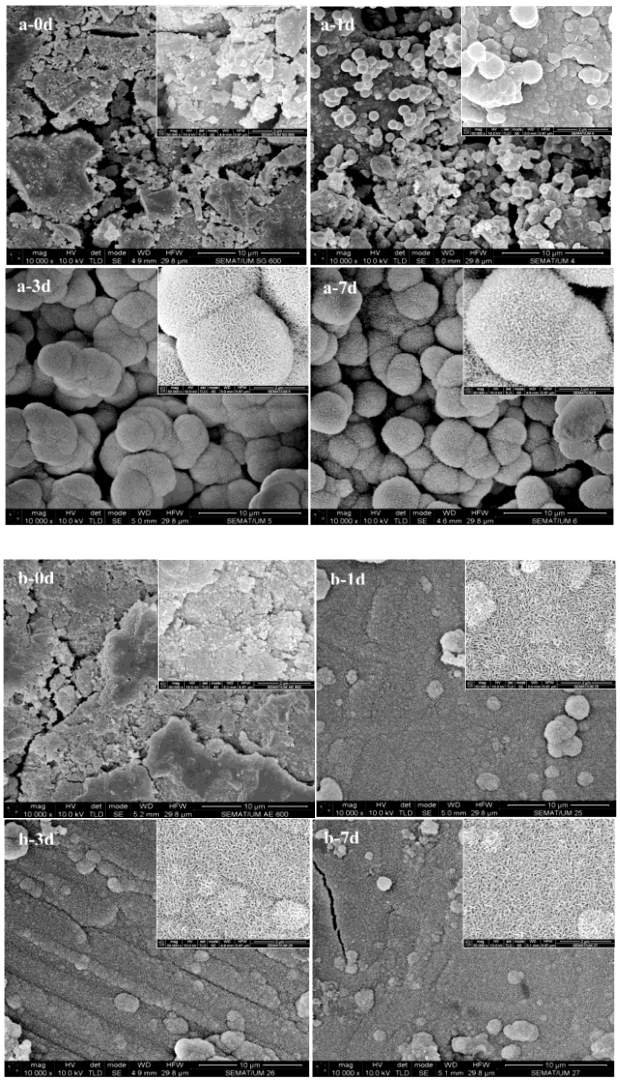

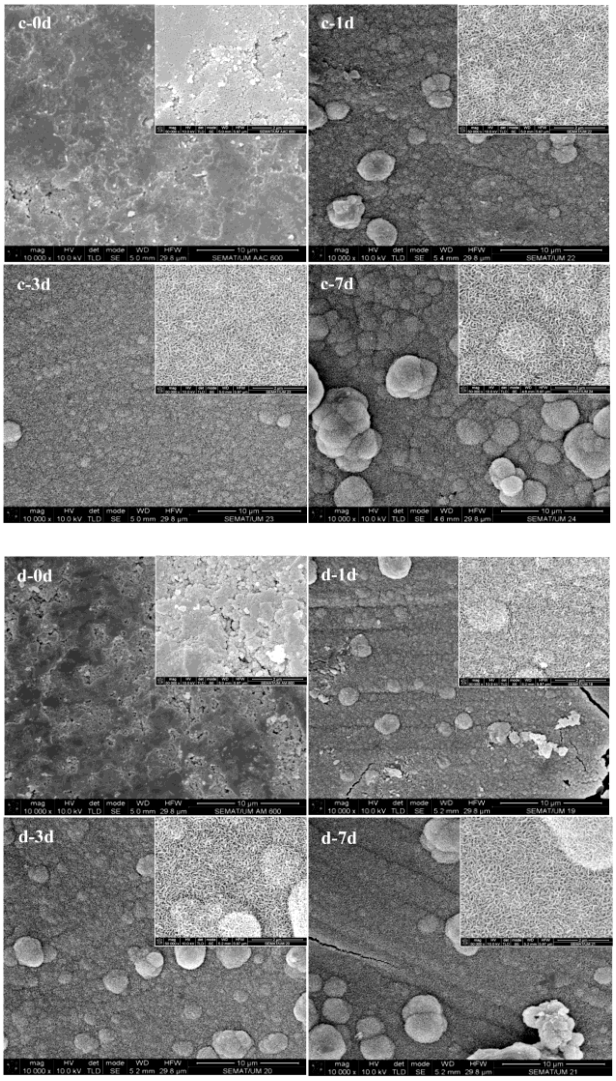

Fig. 7. SEM morphologies of the bioactive glass powders before and after soaking in SBF solution for 0, 1, 3 and 7 days: a- XG-BG 600°C, b- AGE-BG 600°C, c- AGA-BG 600°C and d- AGM-BG 600°C.

The formation of bone like apatite layer during bioactivity experiments was also evaluated by examining the change of surface morphology during the incubation in SBF solution. Fig 7 shows the surface morphology of samples before and after soaking in the SBF for 0, 1, 3 and 7 days. The results show that the surface morphology changes with incubation periods. After 1 day soaking in SBF compared to 0 day as control, the surface shows the formation of individual spherical apatite grain for xerogel bioactive glass XG-BG Fig 7 (a-1d) and a fully covered surface with an extensive calcium phosphate precipitate with tiny flak on the shape [31] for aerogels bioactive glass. This layer is more important in the case of bioactive glass prepared with ethanol AGE-BG Fig 7 (b-1d) and acetoneAGA-BG Fig 7 (c-1d) solvents. With increasing incubation periods, the formation of apatite grains also increase. After soaking for 3 days the surface of XG-BG Fig 7 (a-3d) was fully covered by an apatite layer, and this layer was composed of numerous spherical particles. On the other hand, the more growing and the density of the precipitate (apatite layer) in case of aerogelsbioactive glass fig 7 ((b-3d), (c-3d) and (d-3d)) increased significantly after 7 days of immersion. The ability of aerogels bioactive glass to promote rapid formation of apatite layer after only one day of soaking can be explained by faster interchange between Ca^{2+} ions of the AG-BG and the H_3O^+ from SBF which can give rise to the formation of Si-OH groups on the aerogels bioactive glass surface that induces the apatite nucleation. In addition, the difference on the texture of XG-BG and AG-BG and also the apatite deposition in SBF is extensive in rougher regions and sparse in flatter regions. In the other hand, the rate of apatite formation depends on the texture of samples [31].

4. Conclusion

In this study, a ternary bioactive glasses in the (CaO-P_2O_5-SiO_2) have been successfully synthesized via sol-gel route from two types of gel, xerogel which is the most used in the development of bioactive glasses, and aerogel which is rarely used in synthesizing bioactive glasses with a nano scale sizes.

The results obtained show that the texture of elaborated bioactive glass powders is strongly influenced by two factors, the type of gel used to obtain the bioactive glasses (xerogel or aerogel) and the change of solvent in the case of aerogel (ethanol, methanol or acetone). Aerogels bioactive glass are characterized by less dense and spongy structure with numerous nano scale spherical particles and an excellent bioactivity. An apatite layer was obtained after only one day of immersion in SBF solution unlike to the xerogelbioactive glass which presented a structure more dense and a surface covered with an apatite layer after three days of immersion in SBF.

Acknowledgements

This work was financially supported by the University of Bejaia – Algeria, LaboratoryofEnvironmental Engineering and by the Erasmus Mundus program Battuta which allowed us an internship of ten months in the University of Porto, Department of Metallurgicaland MaterialsEngineering,Faculty ofEngineering.

References

[1]. L. L. Hench, R. J. Splinter, W. C. Allen; T. K. Greenlee. Bonding mechanism at interface of ceramic prosthetic materials. J. Biomed. Mater. Res. 1972; 2: 117-141.

[2]. A. R. Curtis, N.X. West, B. Su. Synthesis of nanobioglass and formation of apatite rods to

occlude exposed dentine tubules and eliminate hypersensitivity. ActaBiomater. 2010; 6: 3740–3746.

[3]. F. Braye, J.L. Irigaray, E. Jallot, H. Oudadesse, G. Weber, N. Deschamps, C. Deschamps, P. Frayssinet, P. Tourermet, H. Tixier, S. Terve, J. Lefaivrell, A. Amirabad. Resorption kinetics of osseous substitute: natural coral and synthetic hydroxyapatite. Biomaterials. 1996; 17: 1345-1350.

[4]. S.H. Jun, E.J. Lee, S.W. Yook, H.E. Kim, H.W. Kim, Y.H. Koh. A bioactive coating of a silica xerogel/chitosan hybrid on titanium by a room temperature sol-gel process. ActaBiomater. 2010; 6: 302-307.

[5]. M. Mehdipour, A. Afshar. A study of the electrophoretic deposition of bioactive glass-chitosan composite coating. Ceram. Int. 2012; 38: 471-476.

[6]. A.M. El-Kady, E.A. Saad, B.M. Abd El-Hady, M.M. Farag. Synthesis of silicate glass/poly(L-lactide) composite scaffolds by freeze-extraction technique: Characterization and in vitro bioactivity evaluation. Ceram. Int. 2010; 36: 995-1009.

[7]. H. Hajiali, S. Karbasi, M. Hossein. H.R. Rezaie. Preparation of a novel biodegradable nanocomposite scaffold based on poly (3-hydroxybutyrate)/bioglass nanoparticles for bone tissue engineering. J. Mater. Sci. - Mater. Med. 2010; 21: 2125-2132.

[8]. C.P. A.T. Klein, Y. Abe, H. Hosono, K.D. Groot. Different calcium, phosphate bioglass ceramics implanted in rabbit cortical bone. An interface study. Biomaterials. 1984; 5: 362-364.

[9]. D. Zhitomirsky, J.A. Roether, A.R. Boccaccini, I. zhitomirsky. Electrophorotic deposition of bioactive glass/polymer composite coating with and without HA nanoparticle inclusions for biomedical applications. J. Mater. Process. Technol. 2009; 209: 1853-1860.

[10]. R. Du, J. Chang. Preparation and characteriwation of bioactive sol-gel-derived $Na_2Ca_2Si_3O_9$. J. Mater. Sci. - Mater. Med. 2004; 15: 1285-1289.

[11]. A. Bachar, C. Mercier, A. Tricoteaux, A. Leriche, C. Follet. M. Saadi, S. Hampshire. Effects of addition of nitrogen on bioglass properties and structure. J. Non-Cryst. Solids. 2012; 358: 693–701.

[12]. T. Krnprobst, J. Plank. Synthesis and properties of magnesium carbonate xerogels and aerogels. J. Non-Cryst. Solids. 2013; 361: 100–105.

[13]. N. Job, A.Théry, R. Pirard, J. Marien, L. Kocon, J. N. Rouzaud, F. Béguin, J. P. Pirard. Carbon aerogels, cryogels and xerogels: Influence of the drying method on the textural properties of porous carbon materials. Carbon. 2005 ; 43 : 2481–2494.

[14]. A. Saboori, M. Rabiee, F. Moztarzadeh, M. Sheikhi, M. Tahriri, M. Karimi. Synthesis, characterization and in vitro bioactivity of sol-gel-derived SiO_2-CaO-P_2O_5-MgO bioglass. Mater. Sci. Eng., C. 2009; 29: 335-340.

[15]. T. Kokubo. Surface chemistry of bioactive glass-ceramics. J. Non-Cryst. Solids. 1990; 120: 138-5.

[16]. W. Zhao, J. Wang, W. Zhai, Z. Wang, J. Chang. The self-setting properties and in vitro bioactivity of tricalcium silicate. Biomaterials. 2005; 26: 6113-6121.

[17]. A. Doostmohamadi, A. Monshi, M. H. Fathi, S. Karbasi, O. Braissant, Q. U. Daniels. Direct cytotoxicity evaluation of 63S bioactive glass and bone-derived hydroxyapatite particles using yeast model and human chondrocyte cells by microcalorimetry. J. Mater. Sci. - Mater. Med. 2011; 22: 2293-2300.

[18]. A. Balamurgan, G. Balossier, D.L. Maquin, S. Pina, A.H.S. Rebelo, J. Faure, J.M.F. Ferreira. An in vitro biological and anti-bacterial study on a sol-gel derived silver-incorporated bioglass system. Dent. Mater. 2008; 24: 1343-1351.

[19]. J.P. Nayak, S. Kumar, J. Bera. Sol-gel synthesis of bioglass-ceramics using rice husk ash as a source for silica and its characterization. J. Non-Cryst. Solids. 2010; 356: 1447-1451.

[20]. L. Radev, K. Hristova, V. Jordanov, M.H.V. Fernandes, I.M.M. Slvado. In vitro bioactivity of 70 Wt.% SiO_2- 30 Wt.% CaO sol-gel glass, doped with 1,3 and 5 Wt.% NbF_5. Cent. Eur. J. Chem. 2012; 10: 137-145.

[21]. A. Rainer, S.M. Giannitelli, F. Abbruzzese, E. Traversa, S. Licoccia, M. Trombetta. Fabrication of bioactive glass-ceramic foams mimicking human bone portions for regenerative medicine. ActaBiomater. 2008; 4: 362-369.

[22]. J.Ma, C.Z. Chen, D.G. wang, X.G. Meng, J.Z. Shi. Influence of the sintering temperature on the structural feature and bioactivity of sol-gel derived SiO_2-CaO-P_2O_5bioglass. Ceram. Int. 2010; 36: 1911-1916.

[23]. A.L. Girot, F.Z. Mezahi, M. Mami, H. Oudadesse, A. Harabi, M.L. Floch. Sol–gel synthesis of a new composition of bioactive glass in the quaternary system SiO2–CaO–Na2O–P2O5 Comparison with melting method. J. Non-Cryst. Solids. 2011; 357 : 3322–3327.

[24]. P. Jiang, H. Lin, R. Xing, J. Jiang, F. Qu. Synthesis of multifunctional macroporous-mesoporous TiO_2-bioglasses for bone tissue engineering. J. Sol-Gel Sci. Technol. 2011.

[25]. H.S. Costa, M.F. Rocha, G.I. Andrade, E.F. Barbosa-Stancioli, M.M. Pereira, R.L. Orefice, W.L. Vasconcelos, H.S. Mansur. Sol-gel derived composite from bioactive glass-polyvinyl alcohol. J. Mater. Sci. 2008; 43: 494-502.

[26]. C.Y. Kim, A.E. Clark, L.L. Hench. Early stages of calcium-phosphate layer formation in bioglasses. J. Non-Cryst. Solids. 1989; 113: 195-202.

[27]. J. Ma, C.Z. Chen, D.G. wang, J.H. Hu. Synthesis, characterization and in vitro bioactivity of

magnesium-doped sol-gel glass and glass-ceramics. Ceram. Int. 2011; 37: 1637-1644.

[28]. E.V. tarasyuk, O. A. Shilova, A. M. Bochkin, A. D. Pomogailo. Investigation into the influence of organic modifiers and ultradispersed hybrid fillers on the structure and properties of glass-ceramic coating prepared by the sol-gel method. Glass Phys. Chem. 2006; 32: 439-447.

[29]. A.R. Boccaccini, M. Erol, W.J. Stark, D. Mohn, Z. Hong, J.F. Mano. Polymer/bioactive glass nanocomposites for biomedical applications: A review. Compos. Sci. Technol. 2010; 70: 1764-1776.

[30]. H.A. Elbatal, M.A. Azooz, E.M.A. Khalil, A.S. Monem, Y.M. Hamdy. Characterization of some bioglass-ceramics. Mater. Chem. Phys. 2003; 80: 599-609.

[31]. A. Balamurugan, G. Balossier, S. Kannan, J. Michel, A.H.S. Rebelo, J.M.F. Ferreira. Development and in vitro characterization of sol-gel derived $CaO-P_2O_5-SiO_2$-ZnO bioglass. ActaBiomater. 2007; 3: 255-262.